Journal of Structural Geology, Vol. 11, No. 7, pp. 815 to 825, 1989
Printed in Great Britain

0191-8141/89 $03.00+0.00
Pergamon Press plc

Experimental studies of compaction and dilatancy during frictional sliding on faults containing gouge

CAROLYN A. MORROW and JAMES D. BYERLEE

U.S. Geological Survey, Menlo Park, CA 94025, U.S.A.

(*Received* 26 *August* 1988; *accepted in revised form* 6 *April* 1989)

Abstract—Transient strength changes are observed in fault gouge materials when the velocity of shearing is varied. A transient stress peak is produced when the strain rate in the gouge is suddenly increased, whereas a transient stress drop results from a sudden change to a slower strain rate. We have studied the mechanism responsible for these observations by performing frictional sliding experiments on sawcut granite samples filled with a layer of several different fault gouge types. Changes in pore volume and strength were monitored as the sliding velocity alternated between fast and slow rates. Pore volume increased at the faster strain rate, indicating a dilation of the gouge layer, whereas volume decreased at the slower rate indicating compaction. These results verify that gouge dilation is a function of strain rate. Pore volume changed until an equilibrium void ratio of the granular material was reached for a particular rate of strain. Using arguments from soil mechanics, we find that the dense gouge was initially overconsolidated relative to the equilibrium level, whereas the loose gouge was initially underconsolidated relative to this level. Therefore, the transient stress behavior must be due to the overconsolidated state of the gouge at the new rate when the velocity is increased and to the underconsolidated state when the velocity is lowered. Time-dependent compaction was also shown to cause a transient stress response similar to the velocity-dependent behavior. This may be important in natural fault gouges as they become consolidated and stronger with time. In addition, the strain hardening of the gouge during shearing was found to be a function of velocity, rendering it difficult to quantify the change in equilibrium shear stress when velocity is varied under certain conditions.

INTRODUCTION

To STUDY the velocity dependence of strength in geologic materials, a variety of frictional sliding experiments have been conducted on rocks and fault gouge. See, for example, Scholz & Engelder (1976), Dieterich (1978, 1981), Hungr & Morgenstern (1984), Solberg & Byerlee (1984) and Shimamoto (1986). These works and others report a range of frictional behavior, including both velocity strengthening (increased strength with higher velocity) and velocity weakening. In spite of these differences, certain observations are consistent throughout. For instance, regardless of the equilibrium value of shear stress after a velocity change, there exists a stress transient before the final stress value is attained. For velocity increases, this transient appears as a stress peak which decays to the new equilibrium value. Conversely, if the velocity suddenly decreases, the stress drops sharply and then gradually rises to the final value. This behavior is incorporated into velocity- and time-dependent frictional models in a number of ways. See, for example, Prevost & Hoeg (1975), Stuart (1979), Rice & Ruina (1983), Gu *et al.* (1984) and Okubo & Dieterich (1986).

Morrow *et al.* (1986) found that the stress transient observed during frictional sliding experiments on Ottawa sand were linked to pore volume changes in the sand layer. Pore volume increased when the stress rose suddenly, and decreased when the stress dropped. An increase in pore volume is evidence of dilation in the sample, whereas a decrease in volume indicates compaction. Thus dilatancy and compaction must be key aspects of the velocity-dependent stress behavior. This paper expands upon that previous work to further investigate the physical mechanism responsible for the stress transients. We report on frictional sliding experiments conducted on crushed Westerly granite to compare the behavior of a monomineralic gouge (Ottawa sand) with one containing many different mineral phases. Frictional sliding experiments were also conducted on crushed quartzite samples to compare the shear stress and dilatancy behavior of an angular quartz gouge with the more spherical grains of Ottawa sand. In addition, we discuss why the equilibrium shear stress after the observed stress transients is difficult to establish in rocks that display pronounced velocity-dependent strain hardening or displacement-dependent strength.

PROCEDURE

A cylindrical sample of Westerly granite, 190 mm long and 76 mm in diameter, was cut at an angle of 30° to the sample axis. The surfaces were ground flat and sand blasted to give an average roughness of approximately 0.06 mm. The two halves were then saturated with deionized water and separated by a 3 mm thick layer of artificial fault gouge. A small hole through the center of each granite piece ensured adequate communication of the fluid in the gouge layer with the rest of the pore pressure system. A porous plug along the sliding surfaces prevented particles from entering the holes. This rock–gouge assembly was jacketed in polyurethane tubing as shown in Fig. 1.

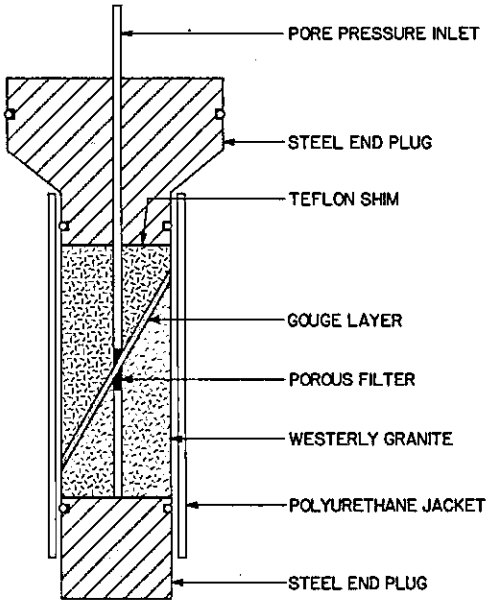

Fig. 1. Sample assembly. The cylinder of granite is 190 cm long and the gouge layer is 3 mm thick.

The first series of experiments was conducted on layers of Ottawa sand, crushed quartzite (Death Valley) and crushed Westerly granite. The gouges were sieved such that all grains were between 500 and 710 μm in diameter. The samples were deformed at a displacement rate of 2.2×10^{-4} mm s^{-1} along the gouge layer during the first 2 mm of axial shortening. Thereafter, this rate was alternated between 2.2×10^{-3} and 2.2×10^{-5} mm s^{-1} every few millimeters by computer-controlled commands until a total displacement of 16 mm had been achieved along the gouge layer. These displacement rates correspond to strain rates along the axis of the rock cylinder (the direction of loading) of 10^{-5} and 10^{-7} s^{-1}, respectively. The experiments were run at constant normal stresses of 17.5, 30, 55 and 105 MPa, and a constant pore pressure of 5 MPa, resulting in effective normal stresses of 12.5, 25, 50 and 100 MPa. The results are referred to by these effective stresses. In this triaxial system the confining pressure was computer controlled so that the normal stress was kept constant as the area of contact decreased. As a result, confining pressure decreased gradually throughout the experiment. Pore volume changes within the gouge were determined by measuring the change in the volume of the fluid reservoir required to maintain constant pore pressure. The pore volume measurements are not affected by the small offsets at the tips of the sample that grow progressively with sliding. Weeks (1980) conducted experiments to compare the volume change in gouge-filled samples that were jacketed with both gum rubber and polyurethane. The gum rubber is very weak and will completely conform to the shape of the sample under pressure. There was no difference in the pore volume response of these tests, verifying that the polyurethane also conforms to the shape of the sample under pressure, without leaving a fluid-filled gap between the jacket and the rock. In the first series of 12 experiments, we compare the effects of effective pressure, grain angularity (Ottawa sand vs crushed quartzite) and mineral composition (Westerly granite vs quartzite) when observing the stress and pore volume response to a sudden velocity change. Grain size and petrographic studies were conducted on the run products of the samples.

In a second series of experiments, the same three gouges were sheared at a displacement rate along the gouge layer of 2.2×10^{-4} mm s^{-1} (10^{-6} s^{-1} axial strain rate) for a total of 16 mm. Effective normal stress was maintained at 50 MPa. At selected intervals during the experiments, the piston was held fixed for periods of time increasing in duration by an order of magnitude from 10 to 100,000 s. Here again, pore volume and stress changes were monitored. In these experiments, time-dependent compaction of the gouge was investigated.

The third set of experiments, conducted only on crushed Westerly granite, consisted of uninterrupted shearing at a constant displacement rate of 2.2×10^{-3} and 2.2×10^{-5} mm s^{-1} (10^{-5} and 10^{-7} s^{-1} axial strain rate) at 50 MPa effective normal stress. Here we observed the effect of velocity on the degree of strain hardening.

Since the force on the piston has been measured outside of the pressure vessel, corrections must be made for the friction of the rubber seals against the piston, which is a function of confining pressure. These corrections have been incorporated into all of the data. In addition, there are corrections for the change in friction ($\Delta\mu$) due to velocity dependence of the rubber seals, sample-end friction and jacket strength which are on the order of 0.0025 at 12.5 MPa, 0.0017 at 25 MPa, 0.0010 at 500 MPa and 0.0007 at 100 MPa for a one decade change in velocity. These values correspond to shear stress reductions of around 0.03, 0.04, 0.05 and 0.07 MPa, respectively, which are small compared to the total stress on the samples and are not discernible on the data plots. These corrections will be discussed in a forthcoming paper. Over 60 frictional sliding experiments were conducted in all to test reproducibility, sources of error and other aspects of material behavior not reported in detail here. All pressure measurements were accurate to ± 0.1 MPa and volume measurements to ± 0.0002 cm^3.

RESULTS

(a) *Stepping experiments*

Shear stress and pore volume data as a function of displacement along the gouge layer are shown in Figs. 2–4 for the first series of velocity-stepping experiments. The initial part of the stress curve is predominantly the elastic response of the entire sample. The overall strength level increased systematically with normal stress as expected. Each sample showed a similar transient stress behavior at the onset of a new sliding velocity. When stepping to the faster velocity, stress rose to a peak and then decayed to a new, higher equilibrium value. When the velocity was suddenly decreased, the

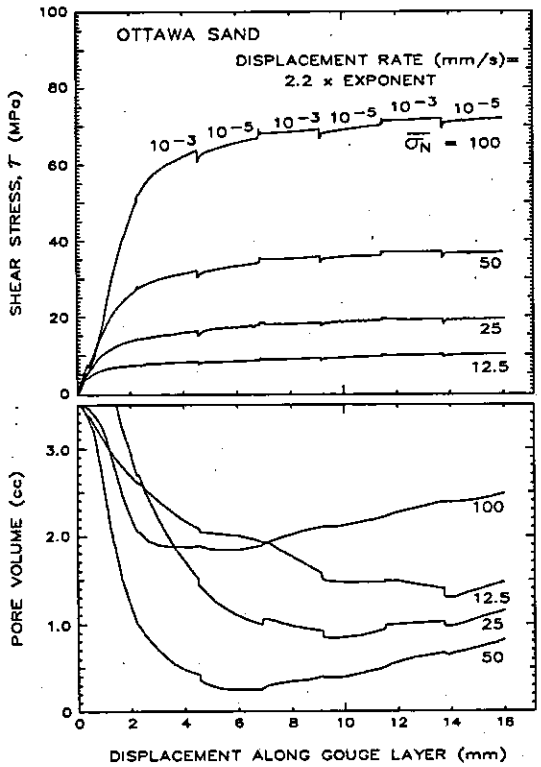

Fig. 2. Shear stress and pore volume as a function of displacement for the Ottawa sand gouge, from Morrow *et al.* (1986). Strain rates are indicated above the stress curves. The initial pore volume is arbitrary.

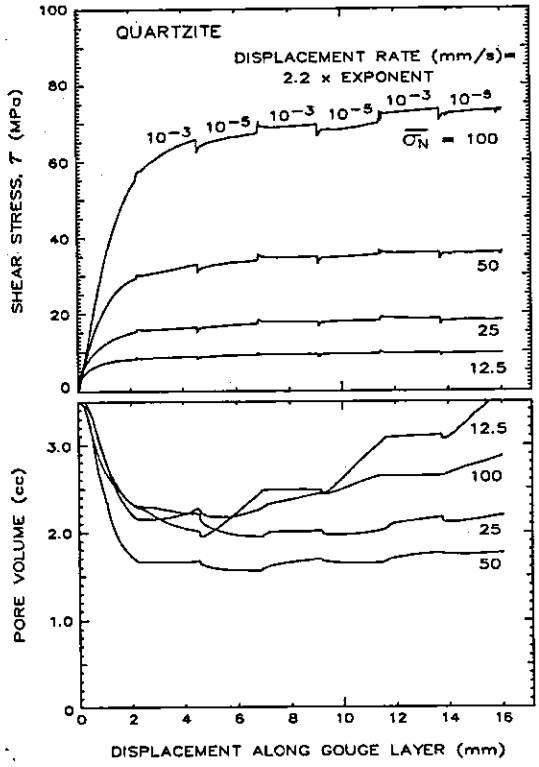

Fig. 3. As Fig. 2 for crushed quartzite.

stress dropped sharply and then rose asymptotically to a lower equilibrium value. The magnitude of the stress transients increased proportionally with the increase in normal stress.

Because the equilibrium strengths of the samples (i.e. after the transient has died away) were slightly higher at the faster slip velocities, they are defined as having a positive velocity dependence. (Conversely, a decrease in strength at the faster slip velocity would be defined as a negative velocity dependence.) The crushed quartzite displayed the most pronounced positive velocity dependence of the three gouge types (Fig. 3), although the Ottawa sand was also clearly positive (Fig. 2). Westerly granite typically displayed the least distinct changes in equilibrium shear stress (Fig. 4). We have not attempted to tabulate these velocity-dependent stress changes (B values, as defined in Dieterich 1978), because all three gouges exhibited a strain hardening that is inversely related to sliding velocity. This leads to difficulties in comparing the steady state stress levels, because they are not simply parallel curves that are offset by an easily measurable amount. Figure 5 shows a more detailed view of the stress data at 50 MPa for the three gouges. Note that the slopes of the stress–strain curves are steeper at the slower rate than at the faster rate. The differences in the stress levels will depend on how far the samples have slid. The most extreme consequence of this behavior can be seen with the Westerly gouge. Because the overall strength level is fairly constant with displacement compared to the quartz-rich gouges, the superimposed velocity-dependent slopes cause the sample to alternate between strain softening and strain hardening as the rates are varied. In this case, it is impossible to say whether the equilibrium stresses increase or decrease with slip rate, because they cannot be meaningfully compared. The velocity-dependent strain hardening differences become more pronounced at higher pressures and temperatures (Moore *et al.* 1986).

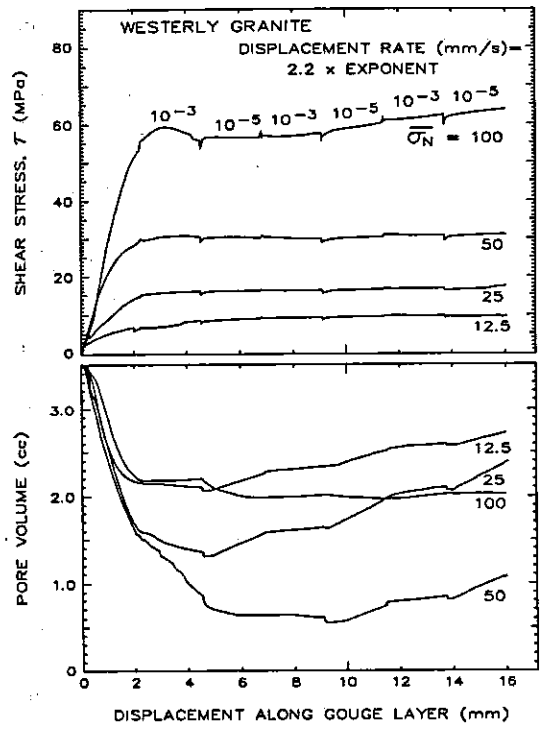

Fig. 4. As Fig. 2 for crushed Westerly granite.

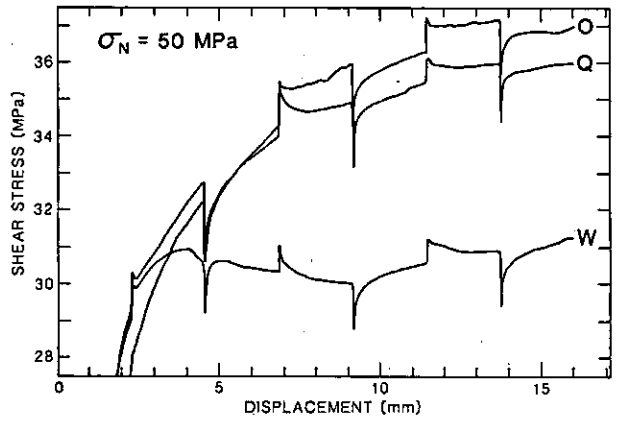

Fig. 5. Enlargement of the shear stress data in Figs. 2–4 at $\sigma_n = 50$ MPa for Ottawa sand (O), crushed quartzite (Q) and Westerly granite (W). Strain rates alternate as indicated in Figs. 2–4.

Several experiments (not reported here in detail) were performed in which three sliding velocities were used in order to approach a particular rate from both faster and slower velocities. This was done because it might be argued that we have not slid far enough to let the transient from a stress peak completely decay away, thereby leading to a possible misinterpretation of the true equilibrium stress level. The results of these experiments show that the strain hardening rate was a function of velocity and was independent of whether sliding was preceded by a stress peak or stress drop.

The pore volume curves for the 12 velocity-stepping experiments all exhibited a characteristic trend with displacement. Volume decreased rapidly with initial compaction, then rose as strain hardening continued. This behavior has been observed and described by Weeks (1980) and Teufel (1981). The slopes of these curves after the initial compaction do not appear to be systematic with confining pressure. This is a further indication that the increase in volume with displacement is not due to a gap between the jacket and the tips of the sample, since the volume in the gap would change with pressure depending on how far the jacket was pushed in. Note that the starting value for the pore volume (3.5 cm^3) was arbitrarily chosen so that the curves could be plotted together. Superimposed on the initial trend of water loss and then gradual volume intake are steps in the pore volume curves which reflect variations in the sliding rate. This pore volume response manifests itself in two ways; as a discrete change at the time of the velocity step, or as a change in the slope of the pore volume curve. Some samples exhibit both types of behavior. Ottawa sand (spherical grains) most clearly shows the former response; pore volume increased slightly at the onset of the faster rate, indicating that the gouge layer had dilated. Conversely, a downward step in pore volume occurred at the start of the slower rate, indicating compaction of the gouge layer. This response shows that compaction and dilation in the gouge layer are a function of strain rate. Healy (1963) also reported a similar relation between dilation and strain rate for Ottawa sand under extremely low pressure (0.06 MPa), but did not relate these changes to variations in shear stress. The volume steps are inversely related to normal stress because the gouge layer must do work against the normal stress in order to expand. For the Ottawa sand at 12.5 MPa, the difference in the pore volume between the two velocities was as much as 0.1 cm^3. This value diminished to 0.05 cm^3 at 25 MPa, 0.025 cm^3 at 50 MPa and about 0.01 cm^3 at 100 MPa.

The initially angular gouges, crushed Westerly granite and crushed quartzite, generally exhibited this dilation and compaction at the velocity steps, but also showed the second type of behavior described above; a pronounced change in slope that was remarkably consistent as the strain rate alternated. Note that within each run (after the initial compaction) the pore volume slopes at 2.2×10^{-3} mm s^{-1} are very nearly the same, as are the

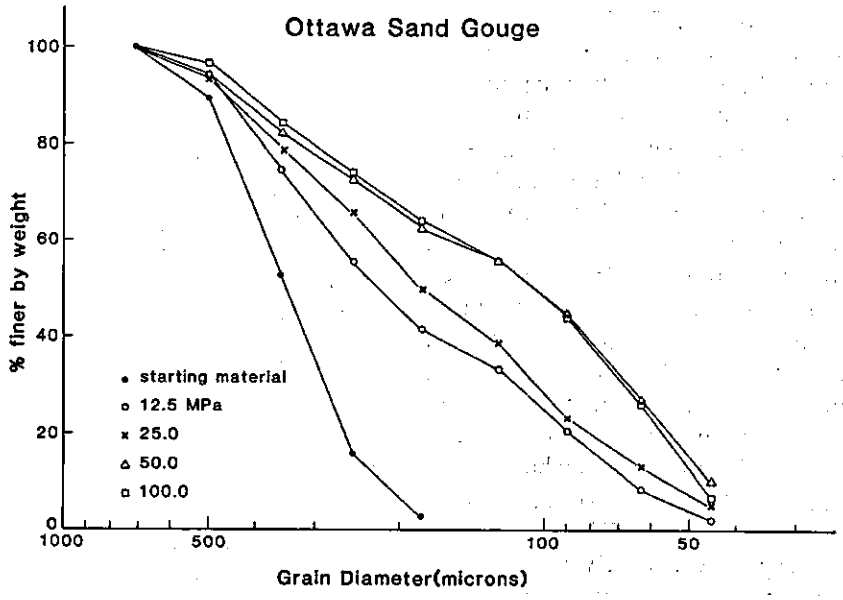

Fig. 6. Grain size analysis of the Ottawa sand gouge after the velocity-stepping experiments illustrated in Fig. 2.

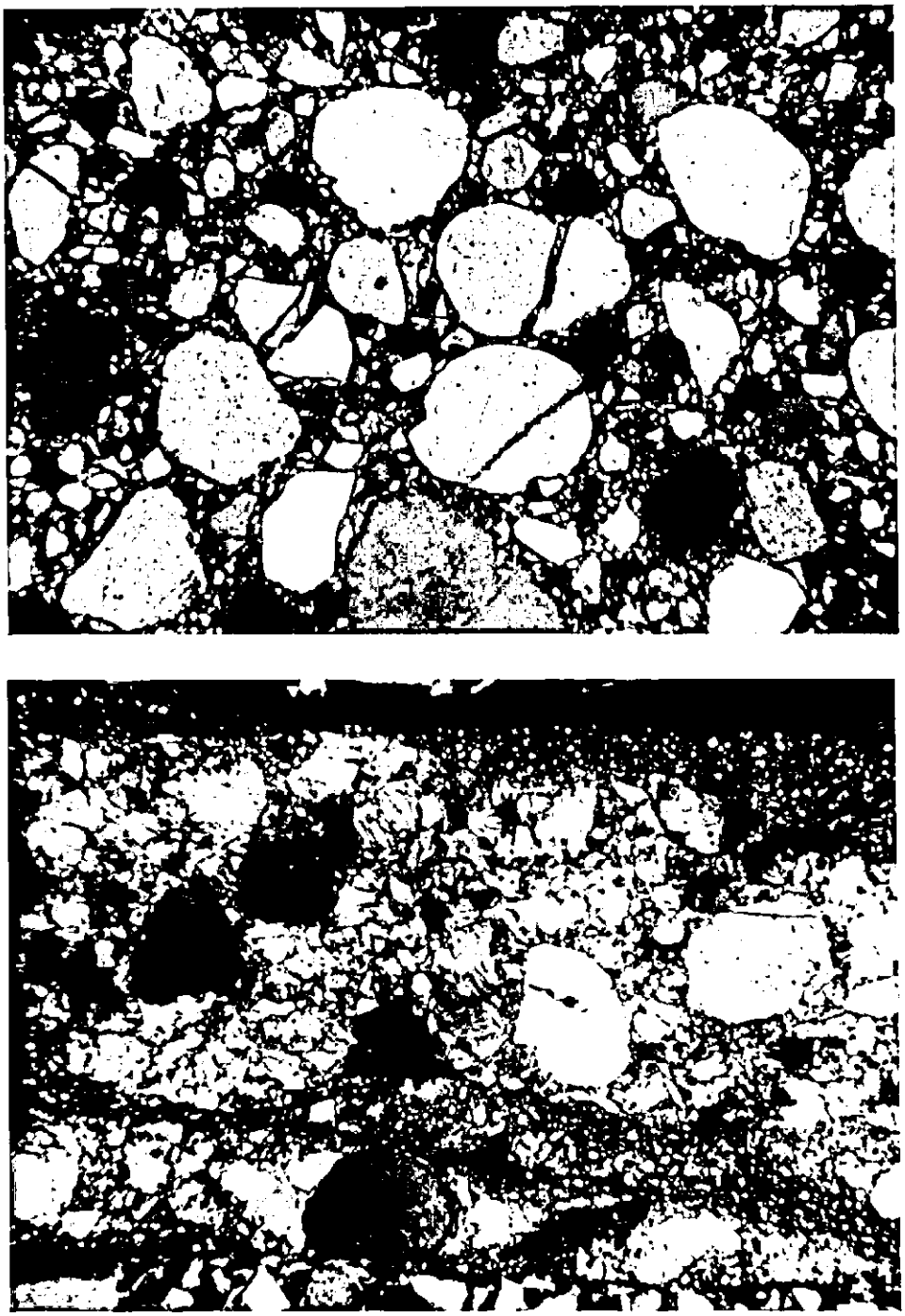

Fig. 7. (a) Photomicrograph of the Ottawa sand gouge (view parallel to the sliding surface), after the velocity-stepping experiment at 12.5 MPa. The image is 3.5 mm across. The gouge layer is uniformly deformed. (b) Photomicrograph of the Ottawa sand gouge (cross-sectional view) after velocity stepping at 100 MPa. The image is 3.5 mm across. The gouge–rock interfaces run horizontally along the top and bottom. The sense of shear is right-lateral as in (a). R_1 shear bands are prominent throughout the length of the gouge layer.

slopes at 2.2×10^{-5} mm s^{-1}. That is to say, the dilatancy rate is the same for a given strain rate, and is independent of displacement. Therefore, grain comminution and the formation of grain fabric during shearing are not factors affecting this behavior.

Grain size analysis and petrographic observations (both perpendicular and parallel to the plane of shearing) were conducted on the run products to investigate the differences in behavior. Grain size determinations of the Ottawa sand by dry sieving are shown in Fig. 6 for the starting material and for the four velocity-varying experiments. The starting material was composed almost entirely of well rounded grains between 200 and 700 μm in diameter. After sliding the grain size distribution covered a much broader range due to the generation of finer particles. The median size shifted from about 340 μm in the fresh material to between 110 and 220 μm after deformation, depending on pressure. The percentage of larger grains present after each experiment was closely ordered according to applied normal stress, because fewer of the initially spherical grains survived at each higher pressure. However, some large grains remained even at 100 MPa due to the large gouge thickness relative to the diameter of the grains. In contrast, the finer fractions do not correlate well with normal stress, possibly because of the increasing difficulty in measuring the finest particles as accurately as the larger ones.

Petrographic observations of the Ottawa sand gouge corroborate the grain size and strength trends described above. At the lowest pressure (12.5 MPa), the different grain size fractions are uniformly distributed throughout the gouge zone (Fig. 7a, view along the plane of shearing). Unbroken grains are easy to distinguish because of their well-rounded nature, compared to the more angular, fractured grains. About 10% of the large grains contain straight, through-going fractures, clearly visible in Fig. 7(a). Very few of the grains contain strain shadows due to the applied pressure.

At 25 MPa, fewer of the large grains remain. The distribution of sizes is still uniform across the thickness of the gouge zone and no distinct texture has developed. However, fracture planes can be traced across the sample in many different orientations. Using the notation of Logan *et al.* (1979) shown in Fig. 8, these planes are identified as R_1, R_2, X and P. No particular orientation is more prevalent than another. At 50 MPa strain shadows are common in the intact grains. The grain texture is no longer homogeneous; uncrushed particles are now concentrated near the center of the gouge zone with finely fractured particles aligning the sides adjacent to the rock interfaces. Shear bands composed of highly comminuted particles have formed in the Y and R_1 planes. These bands have a distinct thickness to them, unlike the straight, two-dimensional fracture planes observed at the lower pressures. At 100 MPa (Fig. 7b), the deformation texture is well established. The most prominent features are numerous R_1 shear bands of finely crushed material occurring at angles of 10–20° to the rock interface. R_2, P and X fracture planes can still be traced across the gouge layer, although these are secondary in significance and do not contribute to the overall deformation texture.

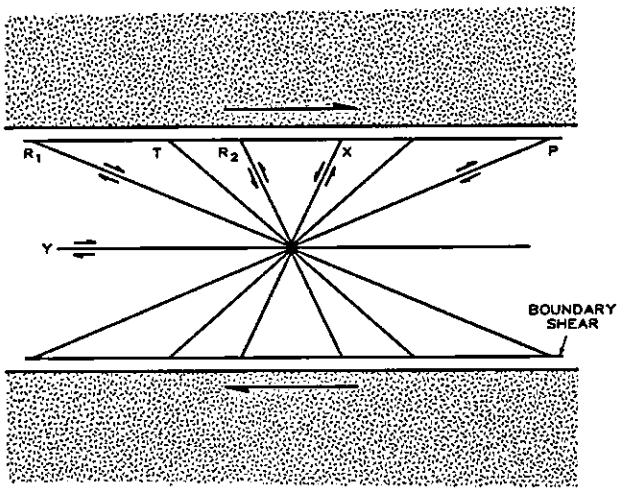

Fig. 8. Cross-sectional view of fracture planes developed in a gouge layer deformed under triaxial conditions. After Logan *et al.* (1979).

The progression of deformation features described above for Ottawa sand was identical to that observed with the crushed quartzite samples at each higher confining pressure. To summarize, both of these quartz-rich gouges exhibited a homogeneous texture at the two lowest pressures, in spite of considerable grain size reduction. At 50 MPa shear localization was more evident, with differentiated zones of larger grains and areas of highly comminuted particles. At 100 MPa R_1 shear bands at angles of 10–20° to the rock interface dominated the texture. Thin section observations of the Westerly granite were similar to those made on the two quartz gouges at the lower pressures, but shear band development was not as well established at the higher pressures.

The angle of the R_1 shear bands relative to the rock interface has often been a topic of detailed analysis. Moore *et al.* (1986) found that the angle between the shear bands and the slip direction was related to sliding stability and was also a function of strain rate. High-angle shear zones (12–20°) correlated with stick–slip behavior and slower velocities. Because our samples were subjected to alternating strain rates, we have not attempted to interpret the significance of the observed range in R_1 shear angles.

Although the stability of the gouge is related to the behavior of the shear bands in constant-velocity experiments, a comparison of our petrographic and pore volume data shows that dilatancy affects the entire gouge layer. Dilatancy is observed at low pressures where there is no evidence of an inhomogeneous structure and, in fact, it appears to be largely independent of the grain fabric. It follows that at higher pressures the pockets of less deformed grains around the shear bands may be active in the dilation–compaction process along with the shear zone itself, although we have no way of determining the contributions of different portions in these experiments.

(b) *Time-hold experiments*

Results from the 'hold' experiments are shown in Figs. 9–11. During the times that the piston was stationary, shear stress decreased progressively in proportion to the length of the hiatus. When sliding resumed, a transient peak occurred whose height was also proportional to the rest time. No stress peak was observed after the 10-s pause in any of the samples. This time is below the limit for observing such a response under these experimental conditions. The transient stress peaks of the experiments are similar in magnitude and form to those caused by the velocity changes in the first series of experiments. These findings corroborate the results of Dieterich (1981), who studied dry, synthetic granite gouges that were alternatively sheared and held fixed under stress, as in our experiments. He found that strength decreased during the fixed periods and, after sliding was resumed, the transient stress peaks were proportional to the length of the stationary time. In this study, we have also monitored the pore volume, in order to understand how the gouge layer changes as a result of this time-dependent phenomenon. The pore volume plots in Figs. 9–11 have the same general characteristics as in the other shearing experiments: volume decreased with initial loading of the gouge, then rose as shearing initiated and progressed. We have plotted only the lower half of the curves to highlight the changes during the stationary periods. The pore volume responses of the two quartz gouges were quite similar during the rests. Small decreases in pore volume indicate that the gouge was compacting with time. At 10 and 100 s, the volume drop was barely distinguishable from the noise in the data. However, the longer pauses showed progressively greater volume decreases with time, more so in the crushed quartz than in the Ottawa sand. Pore volume did not recover from the pauses as quickly as the stress curve, as was also observed in some velocity-stepping experiments. These pore volume measurements indicate that the transient peaks are related to time-dependent compaction in the gouge layer. A higher level

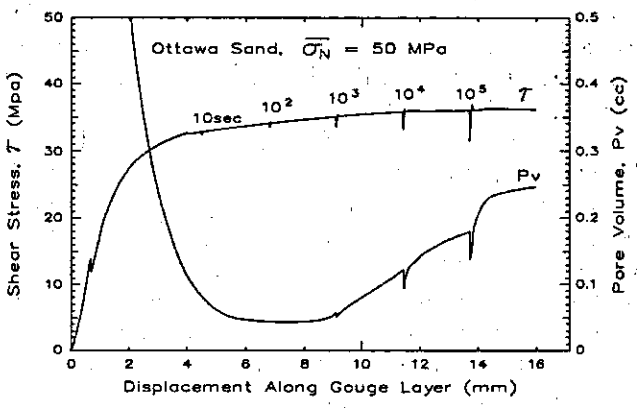

Fig. 9. Shear stress and pore volume change as a function of displacement at a constant strain rate of 10^{-6} s^{-1} for the Ottawa sand gouge from Morrow *et al.* (1986). Rest durations are indicated above the stress curve. Pore volume axis (arbitrary zero) has been magnified to highlight the changes during the pauses.

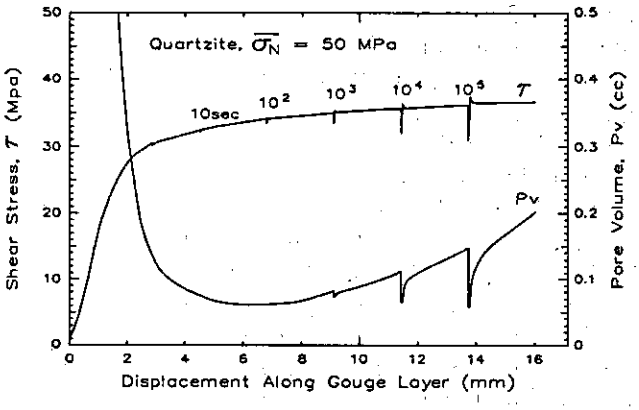

Fig. 10. As Fig. 9 for crushed quartzite.

of stress was required to initiate sliding after each longer hiatus, resulting in progressively larger stress transients. This would imply that the gouges became slightly stronger due to the time-dependent compaction, a phenomenon that is commonly observed in soil mechanics tests.

The results for Westerly granite were most unexpected (Fig. 11). During the hold times, the volume did not decrease, indicating that the gouge did not undergo compaction. However, when sliding continued, the sample dilated in the same manner as the quartz gouges, giving the pore volume curve the appearance of always dilating. It was determined that this response was not due to a leak in the pore pressure system, which could lead to the observed results. If this were the case, then each step would be 10 times larger than the last. Repeated experiments proved that the behavior was reproducible. It is not clear why the Westerly sample behaved in this fashion, because the results of the stepping experiments showed that the gouge compacted in the same way as the quartz samples.

(c) *Constant velocity*

The results of the constant velocity tests are shown in Fig. 12. These two runs exhibit a dip in the stress–strain curve at around 6–8 mm displacement that is typical of Westerly granite (see also Fig. 4), but not of the quartz gouges. Strain hardening in the latter portion of the curve was greater at the slower rate: the stress increased

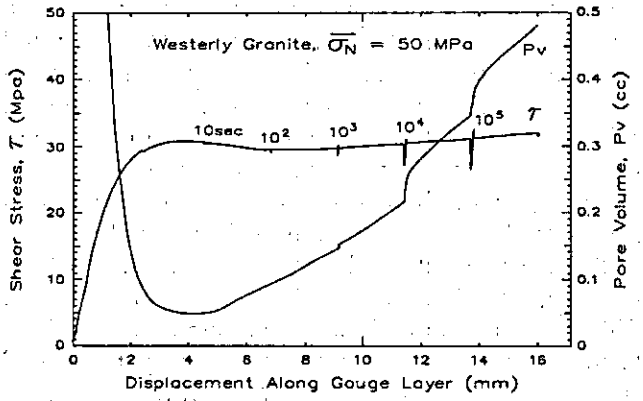

Fig. 11. As Fig. 9 for crushed Westerly granite.

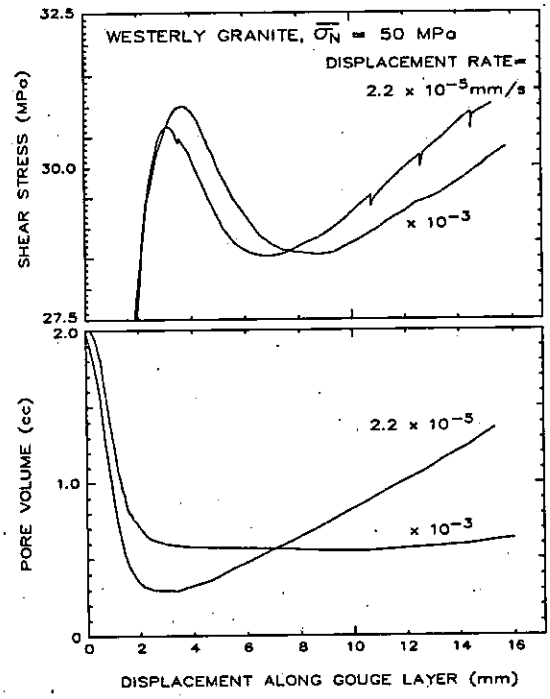

Fig. 12. Shear stress and pore volume as a function of displacement for Westerly granite deformed at constant velocities with no pauses.

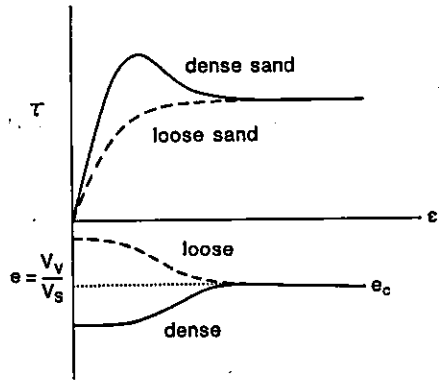

Fig. 13. Idealized stress–strain curves for dense and loosely packed sand (top), and corresponding void ratio plot (bottom). The critical void ratio, e_c, is that value for which the sample neither dilates nor compacts during shearing.

by 0.42 MPa mm^{-1} at 2.2×10^{-5} mm s^{-1} and 0.36 MPa mm^{-1} at 2.2×10^{-3} mm s^{-1}. This corresponds to a $\Delta\mu$ mm^{-1} of 8×10^{-3} and 7×10^{-3}, respectively. The associated pore volume plot clearly shows that the rate of dilation in the gouge is a function of strain rate. The samples dilated more at the slower rate, as with the stepping experiments described earlier. (The flatness at 2.2×10^{-3} mm s^{-1} is due to a small backlash in the pore pressure pump as the piston reverses direction.) In these experiments, the maximum displacement that we could achieve was limited by the geometry of the system. One should not assume that the hardening trend would have continued indefinitely. Some tests at other rates show that this curve starts to flatten off at around 12–14 mm. It would be most interesting to continue shearing to greater displacements, as is possible with the rotary shear machine. However, the rotary geometry also has limitations because of the non-uniform shear stress across the sample. (See Saada & Townsend 1981, for a complete discussion of testing techniques.) Nevertheless, our experiments show that strain hardening is a function of displacement, most probably because of the changing grain size and fabric during shearing.

DISCUSSION

In this paper, we sought to explore the possible effects that grain angularity would have on the stresses and dilatant behavior initially observed with Ottawa sand (Morrow *et al.* 1986). The results of the three series of experiments raise some interesting questions in this regard. We found that the initially angular grains (crushed quartzite and Westerly granite) showed a markedly different pore volume response to changes in sliding velocity compared to the rounder Ottawa sand. However, grain comminution during compaction and shearing would tend to reduce the contrast in grain angularity as shearing progressed. Therefore, one might not expect to see much difference in the response of the gouges if the Ottawa sand eventually resembled the crushed quartzite. In spite of this reasonable assumption, distinct differences in dilatancy rate are apparent in our data. Consequently, there must be some characteristics of the Ottawa sand that are preserved even after 16 mm of shearing. The sieving and petrographic results show that not all of the grains are broken into fine particles by the end of the experiment, even at the highest pressures. Therefore, grain angularity appears to be an important factor influencing the volume response of the gouge.

In spite of the differences in dilatancy rate due to grain angularity, and the puzzling time-dependent compaction differences due to mineral assemblage, the shear stress data for all samples are remarkably consistent. Transient stresses resulted from both velocity- and time-dependent perturbations during shearing. The transient stress behavior observed during the velocity-stepping experiments can be explained by applying some principles of soil mechanics. It has been shown that the strength of a densely-packed sand rises to a peak in stress, followed by a period of strain softening that asymptotically reaches some equilibrium stress value. Conversely, a loosely-packed sand typically shows a gradual increase in stress to the equilibrium frictional value (Das 1983). These two cases are shown schematically in Fig. 13 (top curves). The corresponding void ratio for these two hypothetical soils is shown in Fig. 13 (bottom curves). Void ratio is defined as the ratio of the volume of the voids to the volume of the solids; V_v/V_s. This is a useful parameter in describing the condition of particulate matter because, unlike total volume used in porosity calculations, the volume of the solids does not change as a result of deformation. During the shearing of the dense sand, the increase in void ratio indicated an increase in the volume of the voids, or sample dilation.

For the loose sand, void ratio decreased and the sample compacted. If the initial void ratio were chosen such that there was no change in volume during shearing, this would be called the critical void ratio, e_c, shown in the void ratio plot. This state is eventually attained after continued shearing regardless of the initial condition in this idealized example. Healy (1963) found that the critical void ratio was not a constant for any particular soil, but depended on a number of factors, including normal stress and strain rate.

The dense and loose sands illustrated in Fig. 13 correspond to different consolidation states of the particles. The degree of consolidation in soils is generally defined relative to the past maximum stress, because consolidation is highly dependent on normal stress. However, in these experiments it is more instructive to describe the initial consolidation relative to the consolidation state after the sand has fully adjusted to the applied normal stress and shearing. Hence the dense sand was initially overconsolidated relative to the final equilibrium state, and the loose sand was initially underconsolidated relative to this state. Because Healy (1963) noted that the critical void ratio was a function of velocity, then it follows that consolidation is also a function of velocity. If the sliding velocity were suddenly to change, then the consolidation state must change as well, because the void ratio will adjust to a new equilibrium.

The results of this soil mechanics example can be applied to our experiments to help understand the rate-dependent dilatancy response of the gouge. It would be useful to diverge for a moment and explain why the pore volume response of our samples differs from that shown in Fig. 13. The soil mechanics example is intended to show the response of sand at low pressures in which grains ride over one another rather than break. In this case the void ratio becomes a constant because the grains are not changing their character (becoming smaller, less sorted, angular, etc.), and a steady state is eventually reached. In our higher pressure experiments the grain size, shape and fabric were continually changing due to comminution. The grains were initially well sorted and corresponded to the loose packing shown in Fig. 13. During loading, the grains become more densely packed, not only because the applied pressure forced them into a more dense configuration, but because grains also fractured and smaller particles filled the voids between the larger ones. This resulted in the large volume decreases observed during the initial loading of the samples. Differences in the extent of this volume decrease may be related to variations in the initial density of the sand. After the initial compaction, the samples began to dilate as shown in Fig. 12. Weeks (1980) attributed this dilation to the absorption of water on the surfaces of the fine-grained powder that is produced during shearing. The applied shear stress will also cause voids to open that create a less dense packing of the grains. In addition, the dilatant behavior depends to a certain extent on the degree of sorting, which we have observed is continuously changing. Regardless of the mechanisms involved, the dilatant behavior can be explained by the comminution that occurs at high pressure that is absent in the soil mechanics example of Fig. 13. Therefore, the critical void ratio concept described above must be acting in addition to (or superimposed on) the dilatancy trend observed in our samples. When the sliding velocity suddenly increased in these experiments, the gouge was initially overconsolidated under the new conditions because the grains were more densely packed than they would be under equilibrium. The sample responded by dilating until the critical void ratio for the new rate had been reached. The accompanying transient peak in shear stress is typical of the dense sand behavior described above. Conversely, when the rate decreased, the gouge layer was initially underconsolidated relative to equilibrium at that rate (more loosely packed), and the grains adjusted to the new condition by suddenly compacting, followed by a gradual stress increase typical of the behavior of loose sand. For these experiments the change in void ratio due to the velocity change ranged from 6×10^{-4} to 2×10^{-3}. The details of how dilatancy (or critical void ratio) is a velocity-dependent process are not fully understood at present.

Our first series of experiments demonstrate that velocity-dependent behavior can result in overconsolidation of the fault gouge. In addition, numerous soil mechanics studies have shown that time-dependent compaction can affect granular materials in a similar fashion. This is illustrated in the second series, in which the same Ottawa sand gouge displayed stress transients and strengthening after being held under high stress for various lengths of time. These experiments combine the effects of both time and velocity factors because the transition from sliding to the locked position or vice versa constitutes a velocity change. Time-dependent transient behavior is pertinent to the discussion of fault strength because, in the natural situation, fault zones may become locked for significant periods of time, resulting in a gradual compaction and strengthening of the gouge. The stresses that initiate slip must overcome this effect.

REFERENCES

Das, B. M. 1983. *Advanced Soil Mechanics*. Hemisphere, Washington.

Dieterich, J. H. 1978. Time-dependent friction and the mechanics of stick–slip. *Pure & Appl. Geophys.* **116**, 790–806.

Dieterich, J. H. 1981. Constitutive properties of faults with simulated gouge. In: *Mechanical Behavior of Crustal Rocks* (edited by Carter, N. L., Friedman, M., Logan, J. & Stearns, D.). *Am. Geophys. Un. Geophys. Monogr.* **24**, 102–120.

Gu, J.-C., Rice, J. R., Ruina, A. L. & Tse, S. T. 1984. Slip motion and stability of a single degree of freedom elastic system with rate and state dependent friction. *J. Mech. Phys. Solids* **32**, 167–196.

Healy, K. A. 1963. The dependence of dilation in sand on rate of shear strain. Unpublished D.Sc. thesis, Massachusetts Institute of Technology, Cambridge, Massachusetts.

Hungr, O. & Morgenstern, N. R. 1984. High velocity ring shear test on sand. *Géotechnique* **34**, 415–421.

Logan, J. M., Friedman, M., Higgs, N., Dengo, C. & Shimamoto, T. 1979. Experimental studies of simulated gouge and their application to studies of natural fault zones, Proc. Conf. VIII, Analysis of actual fault zones in bedrock. *U.S. geol. Surv. Open-file Rept* **79-1239**, 305–343.

Moore, D. E., Summers, R. & Byerlee, J. D. 1986. The effect of sliding velocity on the frictional and physical properties of heated fault gouge. *Pure & Appl. Geophys.* **124**, 31–52.

Morrow, C., Lockner, D. & Byerlee, J. 1986. Velocity and time dependent stress transients in simulated fault gouge. *Proc. Int. Symp. on Engineering in Complex Rock Formations*, Beijing, 142–148.

Okubo, P. & Dieterich, J. H. 1986. State variable fault constitutive relations for dynamic slip. In: *Earthquake Source Mechanisms* (edited by Das, S., Boatwright, J. & Scholz, C.). *Am. Geophys. Un. Geophys. Monogr.* **37**, 25–35.

Prevost, J. H. & Hoeg, K. 1975. Soil mechanics and plasticity analysis of strain softening. *Géotechnique* **25**, 279–297.

Rice, J. R. & Ruina, A. L. 1983. Stability of steady frictional slip. *J. appl. Mech.* **105**, 343–349.

Saada, A. S. & Townsend, F. C. 1981. State of the art: Laboratory strength testing of soils. In: *Laboratory Shear Strength of Soil* (edited by Yong, R. N. & Townsend, F. C.). American Society for Testing Materials, ASTM STP 740, 7–77.

Scholz, C. H. & Engelder, T. J. 1976. The role of asperity indentation and ploughing in rock friction, I. Asperity creep and stick–slip. *Int. J. Rock Mech. & Mining Sci. Geomech. Abs.* **13**, 149–154.

Shimamoto, T. 1986. Transition between frictional slip and ductile flow for halite shear zones at room temperature. *Science* **231**, 711–714.

Solberg, P. & Byerlee, J. 1984. A note on the rate sensitivity of frictional sliding of Westerly Granite. *J. geophys. Res.* **89**, 4203–4205.

Stuart, W. D. 1979. Strain softening prior to two-dimensional strike slip earthquakes. *J. geophys. Res.* **84**, 1063–1070.

Teufel, L. W. 1981. Pore volume changes during frictional sliding on simulated faults. In: *Mechanical Behavior of Crustal Rocks* (edited by Carter, N. L., Friedman, M., Logan, J. & Stearns, D.). *Am. Geophys. Un. Geophys. Monogr.* **24**, 135–145.

Weeks, J. D. 1980. Some aspects of frictional sliding at high normal stress. Unpublished Ph.D. thesis, Stanford University, Stanford, California.